Computational Lab 3: Flow Over Thin Airfoils

Connor Ott - 104690690

Introduction

Elementary flows such as Uniform Flow and Vortices are not particularly interesting for flow analysis as these idealized don't actually exist. However, when combined, elementary flows can be used to simulate more complex flows. These more complex flows are much more useful for analysis. This lab aims to construct a simulation for flow over a thin, symmetric airfoil by superimposing elementary flows. In addition, it will analyze how increasing the number of elementary flows used can increase the accuracy of the simulation. Finally, it will observe how the flow changes with different chord lengths, free stream velocities, and angles of attack.

Theory

These elementary flows can be combined because they all satisfy Laplace's Equation. That is, $\nabla^2\phi = 0$ and $\nabla^2\psi = 0$ for any velocity potential, ϕ, or stream function, ψ, corresponding to an elementary flow. Because the Laplacian operator, ∇^2, is a linear operator, any linear combination of elementary velocity potentials or stream functions will satisfy Laplace's equation as well. This means that any flows constructed using superposition of elementary flows have valid velocity potentials and streamline functions.

The flow over a thin airfoil can be simulated using flow over a flat plate. This flow is represented by the combination of uniform flow and a vortex sheet. The vortex sheet is made up of N discrete vortices positioned along the chord line of the thin airfoil. The combined stream functions and velocity potentials simulating flow over a flat plat can then be written as:

$$\psi = \psi_{uniform} + \sum_{i=1}^{N} \psi_{i,vortex} \qquad\qquad \phi = \phi_{uniform} + \sum_{i=1}^{N} \phi_{i,vortex}$$

Substituting in for the individual stream functions and velocity potentials yields Eqs.(1),[1] which approximate the flow over a thin, symmetric airfoil at angle of attack α in a free stream flow with velocity V_∞.

$$\begin{aligned} \psi(x,y) &= V_\infty(y\cos\alpha - x\sin\alpha) + \sum_{i=1}^{N} \frac{\Gamma(x_i)}{2\pi} ln\big(\sqrt{(x-x_i)^2+y^2}\big) \\ \phi(x,y) &= V_\infty(x\cos\alpha + y\sin\alpha) - \sum_{i=1}^{N} \frac{\Gamma(x_i)}{2\pi} \arctan\left(\frac{y}{x-x_i}\right) \end{aligned} \tag{1}$$

In Eqs.(1), the effect of each vortex is dependent on its location along the chord of the airfoil. Each vortex's circulation is defined by Eq.(2), where c is the chord length, and Δx is the fixed distance between vortices. Due to the flat plate approximation, the vortex strength is *only* dependent on the vortex's x-position along the chord, since the chord line is defined along the x-axis, and the vortices lie on the chord. I.e. the y-position of the vortices are always zero. Also, note that Eq.(2) satisfies the Kutta Condition for flow over a solid body, which ultimately dictates that the vortex strength at the trailing edge of an airfoil must be zero. Eq.(2) evaluated at $x = c$ proves this.

$$\Gamma(x) = 2\alpha V_\infty \sqrt{\frac{1-x/c}{x/c}}\Delta x \tag{2}$$

Using Eqs.(1), the velocity field can be determined using the definitions of the streamlines and velocity potential. That is, $u = \partial\psi/\partial y = \partial\phi/\partial x$ and $v = -\partial\psi/\partial x = \partial\phi/\partial y$.[1] Then, in conjunction with Bernoulli's equation, the velocity field can be used to determine the pressure distribution around the airfoil. The results from superposition of the uniform flow and N discrete vortices can be found in the Results section.

Results

Fig.(1) shows how the flow is disturbed by the thin airfoil via stream lines and velocity potential isolines. Here, the streamlines are curves tangent to the flow velocity at every point. The velocity potential isolines or "equipotential" lines indicate lines of equal velocity potential.

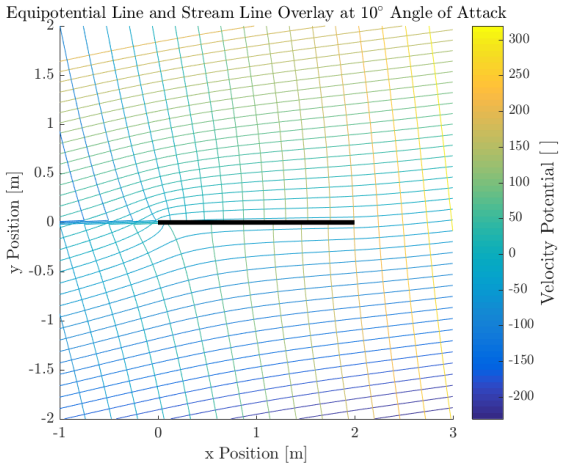

Figure 1. Eqipotential and Stream lines simulated over a flat plate.

Fig.(2) illustrates the pressure distribution in the flow as it passes the plate. This is particularly useful for understanding the lift acting on the plate.

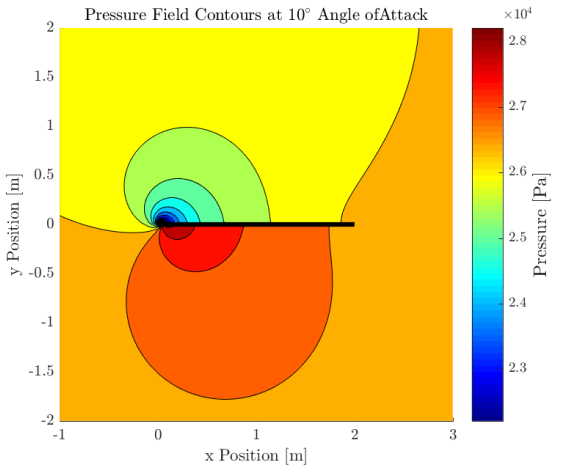

Figure 2. Pressure distribution shown with isobars. Believe it or not, this is how most 70's music artists generated their album covers.

In addition to plotting flow fields around the plate, this lab looked into how error in the simulation changed with increasing the number of vortices used in the simulation. Fig.(3) shows this trend along with fits for to better quantify the results.

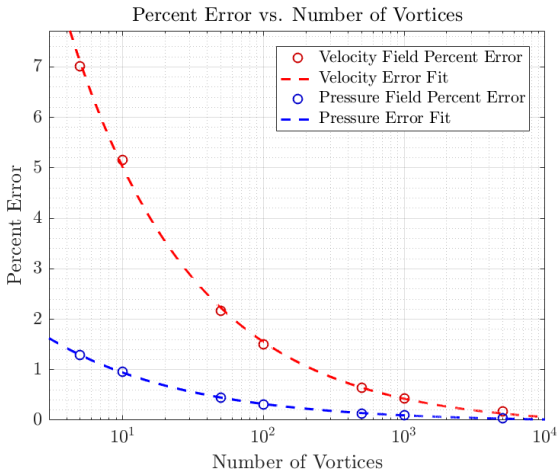

Figure 3. Error trends for increasing number of vortices used in simulation.

Discussion

Looking back at the plots in the Results section allows for some qualitative and quantitative discussion which provides more insight into the properties of the flow, as well as the accuracy of the simulation. Note that, in Fig.(1), at every intersection between a stream line and equipotential line, there forms a right angle. This is consistent with the definitions of stream line and velocity potential. That is, a streamline is tangent to the flow velocity at all points. Since the flow velocity is equal to the gradient of the velocity potential, the stream lines should, at all points, be perpendicular to the velocity equipotential lines. Figures depicting the stream functions and equipotential lines separately can be found in the appendix.

Another, more glaring aspect of Fig.(1) is the discontinuity in the velocity potential at the leading edge of the plate. This not only expected, but necessary to generate lift on the airfoil. Consider the equation for circulation over the closed curve C beginning at point A at the leading edge of the plate, and ending at point B back at the the leading edge. In order to generate lift, the circulation must be non-zero. Eq.(3) indicates how this discontinuity is necessary for non-zero circulation, and subsequently, non-zero lift on a body.[2]

$$0 \neq \Gamma = -\oint_A^B \vec{V} \cdot d\vec{s} = \oint_A^B \nabla\phi \cdot d\vec{S} = \phi(B) - \phi(A) \neq 0 \tag{3}$$

In order to generate lift, $\phi(A)$ and $\phi(B)$ must not have the same value, even though they represent the same point in space. Thus, the discontinuity is necessary to generate lift. For a clearer view of the discontinuity, see the appendix.

Moving on to the pressure distribution plot, it's important to recognize that this data shown in Fig.(2) adds value to the statements in the previous paragraph. The unequal pressure distribution above and below the plate indicates that lift is indeed being generated by this flow.

In addition to Fig.(1), Fig.(7)(located in the appendix) aids in the understanding of the velocity potential. The velocity field shown here indicates that, in addition to flowing perpendicular to equipotential lines, the velocity always points in the direction of increasing velocity potential. This is another consequence of the velocity being equal to the gradient of velocity potential. This plot also show more clearly where stagnation points will occur at higher angles of attack.

The error trend shown in Fig.(3) provides insight to the accuracy of the simulation. This plot was created by generating flows using different numbers of vortices and comparing them to a flow generated with 10^5 vortices. The comparison was made using the Frobenius norm of the difference between the "accepted" and "experimental" flow matrices. The Frobenius norm is way of describing the difference between two matrices in the same way that the Euclidean norm is a way of describing the distance between two points in Cartesian space. The formula used to find the error is shown in Eq.(4).

$$Error = \frac{||X_{N=10^5} - X_{N,Var}||_F}{||X_{N=10^5}||_F} \times 100 \tag{4}$$

Fitting this error trend allowed for a quantitative description for error as a function of N. The following equations are fits generated by MATLAB's *fit* function.

$$E_V = 15.8N^{-0.49} - 0.12$$
$$E_P = 2.7N^{-0.44} - 0.034 \tag{5}$$

Both functions vary approximately with $N^{-\frac{1}{2}}$. With this, it can be gathered that error decreases on the order $O(N^{-\frac{1}{2}})$ for this particular simulation. On a more qualitative note, it can be seen that lower values of N provide sloppier plots and overall poorer representations of flow properties. An example of one of these low-N plots can be found in the Appendix.

Simulations like these allow scientists and engineers to observe how a flow might change without spending time and resources on physical experiments. For instance, with this simulation, varying the angle of attack can drastically change how flow moves around an airfoil. This variation, along with variations in chord length and free stream velocity are shown in Fig.(4).

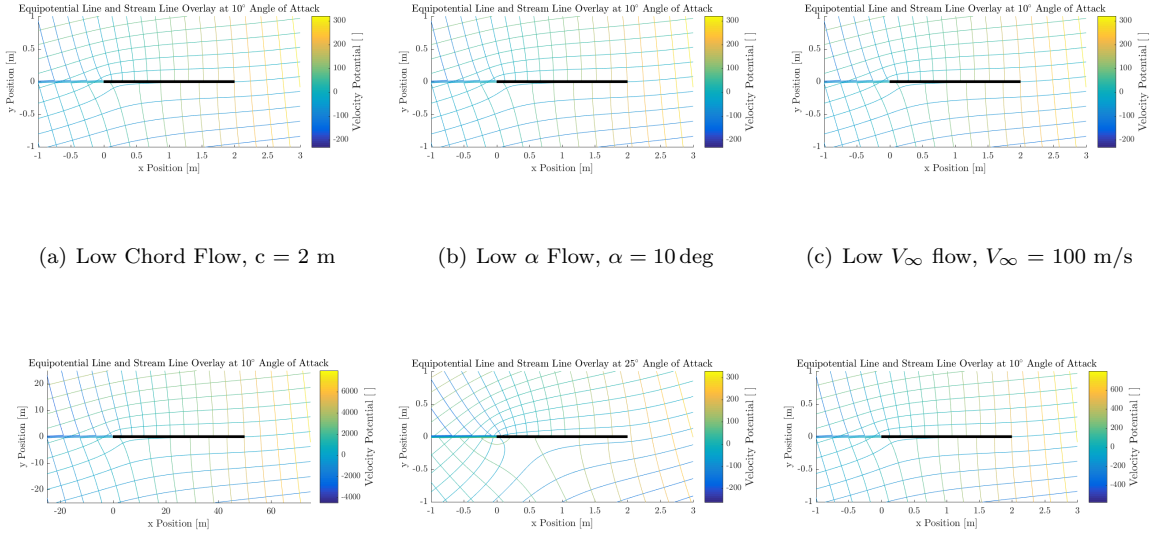

(a) Low Chord Flow, c = 2 m

(b) Low α Flow, $\alpha = 10\,\text{deg}$

(c) Low V_∞ flow, $V_\infty = 100$ m/s

(d) High Chord Flow, c = 50 m

(e) High α Flow, $\alpha = 25\,\text{deg}$

(f) High V_∞ flow, $V_\infty = 250$ m/s

Figure 4. Streamline and Velocity Potential comparisons.

Here it's clear to see that while changing values like chord length and free stream velocity can change values of velocity potential, only changing angle of attack will change its geometry. This is one of the main reasons that wind tunnel testing is a viable source of experimentation for modeling flows. V_∞ and chord length can be scaled up or down with no change to flow geometry. This assumption, however, is only valid in the inviscid, incompressible scenario that this simulation was created for. Large chord lengths will induce large boundary layers in viscous flow, and large velocities will induce compressibility effects and even shock waves in compressible flow. However, for high Reynold's number flows where viscous forces are less pertinent than inertial forces, and low speed flows where incompressibility is a valid assumption ($0.7 < M < 1.2$), wind tunnel testing can be carried out, and the scaling abilities shown in Fig.(4) will hold.

Appendix

Stream functions and equipotential lines on separate plots are shown below.

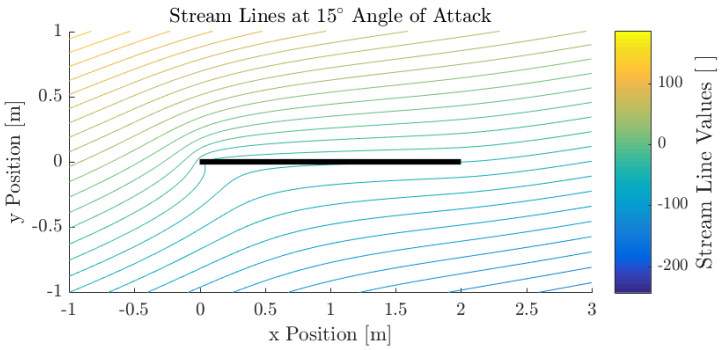

Figure 5. Streamlines for thin plate at 15^{circ} angle of attack

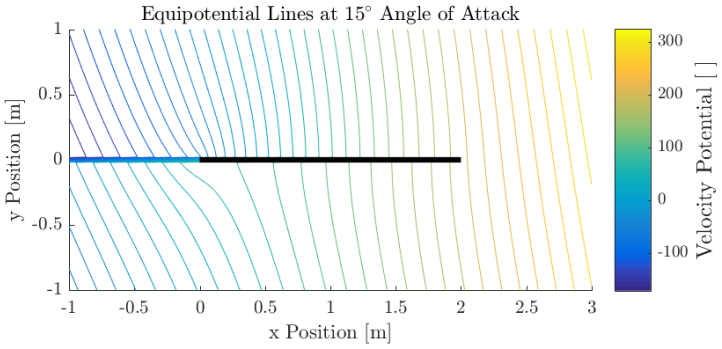

Figure 6. Equipotential lines for thin plate at 15^{circ} angle of attack

Fig.(7) provides more insight to how flow velocities change in relation to changes in velocity potential.

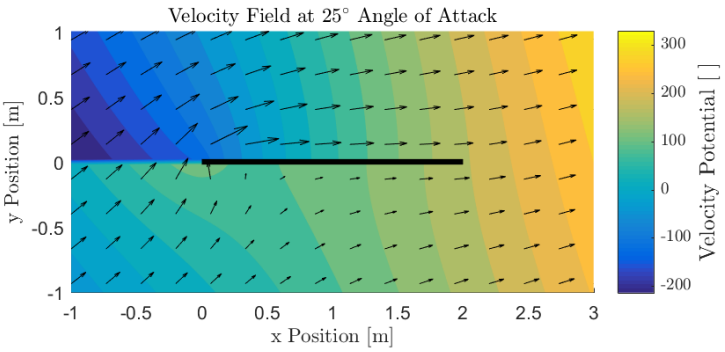

Figure 7. Velocity potential (colormap) overlaid with the velocity field of the flow.

Fig.(8) Indicates low quality plots for small numbers of vortices.

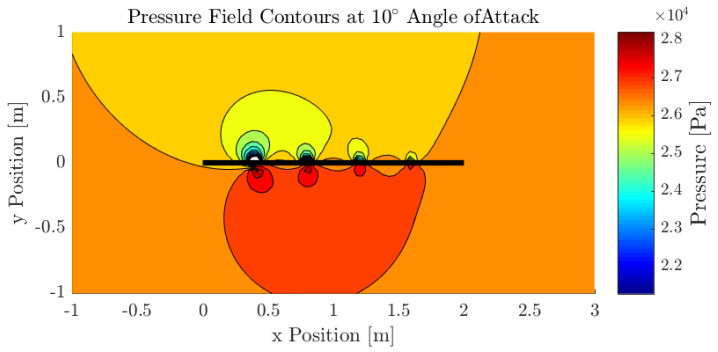

Figure 8. Example of a Low-N pressure contour plot. Here, N = 5 vortces. Notice that the effects of individual vortices can be seen.

References

[1]Anderson, John D. Fundamentals of Aerodynamics. 6th ed., McGraw-Hill Education, 2017.
[2]Thanks to Dr. Evans for his help in explaining the discontinuity in the velocity potential.